Aerosol and Air Quality Research, 18: 79–90, 2018

ISSN: 1680-8584 print / 2071-1409 online
doi: 10.4209/aaqr.2016.12.0548

Characterization and Modeling of Fog in the Mexico Basin

Pohema González-Viveros[1], Ernesto Caetano[2], Fernando García-García[3*]

[1] *Programa de Posgrado en Ciencias de la Tierra, Universidad Nacional Autónoma de México, Ciudad de México 04510, Mexico*
[2] *Instituto de Geografía, Universidad Nacional Autónoma de México, Ciudad de México 04510, Mexico*
[3] *Centro de Ciencias de la Atmósfera, Universidad Nacional Autónoma de México, Ciudad de México 04510, Mexico*

ABSTRACT

The character of fog in a region centered at Mexico City International Airport was investigated using 10 years of historical data. Hourly surface observations, synoptic charts, satellite images and twice-a-day radiosondes were used to identify fog events under the influence of various synoptic and mesoscale features. A quantitative assessment on the likelihood of which mechanisms lead to fog formation was obtained. Also, three fog events (radiation, advection and frontal) were simulated with the Weather Research and Forecasting (WRF) model, and the results were compared to observations. The study included a comparison of the skills of different planetary boundary layer (PBL) and microphysical schemes. A sort of generalization cannot easily be applied, but allows one to determine which parameterizations performed better for each case in a high, tropical region. In general, from the model results for liquid water content, the cloud microphysics WSM3 and PBL Yonsei University schemes reproduced advection and frontal fog events quite well, whereas CAM 5.1 and Quasi-Normal Scale Elimination schemes worked better for radiation fog episodes.

Keywords: Fog types; Fog modeling; Mexico Basin; WRF model.

INTRODUCTION

Fog is a stratiform cloud near the ground that reduces horizontal visibility to less than 1 km (WMO, 1992). This phenomenon plays an important role in the hydrological cycle, but can be also a natural hazard that causes danger for all varieties of air, land and water transportation. Fogs of all types originate when the temperature and dew point of the air become nearly identical. This may occur through cooling of the air to its dew point, or by adding moisture and thereby elevating the dew point. Since fogs are formed primarily through dynamic and adiabatic processes in the boundary layer, their formation, dispersion and decay depend on the balance between condensation in the fog layer, evaporation processes and settling of droplets. Such a balance was noticed by Choularton *et al*. (1981) during a radiation fog field study, and later theoretically confirmed by Zhou and Ferrier (2008). Like most hydrometeorological phenomena, fog occurrence strongly varies with geographical location (Croft *et al.*, 1997), and its observation and recording methods are still very dependent on direct human presence and perception (Lee *et al*., 2010). Despite the numerous field studies and recent advances on instrumentation and remote sensing technologies for fog observations, its numerical modeling and forecasting skills are still limited (Zhou *et al*., 2012). This is mainly due to the complex interactions that occur over various time and space scales among microphysical, thermodynamical and dynamical processes, associated to the great variability of the surface-atmosphere interface and topographic effects (Gultepe *et al.*, 2007). For these reasons, a good understanding of these mechanisms is necessary to develop adequate tools for fog modeling and forecasting. Both one- and three-dimensional models with several combinations of physical and statistical parameterizations are frequently used in fog numerical simulations (Bergot and Guédalia, 1994; Bott and Trautmann, 2002; Steppeler *et al*., 2003; Müller *et al*., 2007). Although mesoscale models – such as the Weather Research and Forecasting (WRF) model – have been mainly concerned with the simulation of advection fogs (Nakanishi and Niino, 2006; Román-Cascón *et al*., 2016), they have been also utilized for modeling radiation-advection (Van der Velde *et al.*, 2010; Román-Cascón *et al.*, 2011), mountain (Shimadera *et al*., 2012), and ice fogs (Gultepe *et al*., 2015). Even though great advances have been accomplished, given the complexity of the problem none of these efforts have been fully successful to simulate all types of fog formation and evolution (Gultepe, 2012). A thorough review on the

* Corresponding author.
Tel.: +52 (55) 5622-4087; Fax: +52 (55) 5616-0789
E-mail address: ffgg@atmosfera.unam.mx

state of the art of fog studies, including simulation and forecasting, is given by Gultepe (2007) and Gultepe *et al*. (2012).

The wide variety of conditions under which fog occurs has been documented using various classifications. The most widely used fog classification system – originally developed by Willett (1928) and later modified and amplified by Byers (1959) – is based on the prevailing synoptic conditions and the main physical processes responsible for its formation. It considers three main types of fogs, each with several sub-types: radiation, advection and frontal fog [see, for example, AMS (2017)]. Radiation fog is produced over a land area when nocturnal radiational cooling reduces the air temperature to or below its dew point, typically under clear skies and weak wind conditions. Advection fog occurs when an air mass moves over a surface with different thermal characteristics, adding water vapor to the air to reach saturation and thus causing condensation near the ground. Frontal fogs are always associated with the passage of either cold or warm fronts, and are the result of vertical mixing of moist air parcels of different temperature.

In Mexico, most existing studies have a regional character in addressing specific aspects of the phenomenon for particular applications. For example, fog in the mountainous, eastern coastal region of the country has been studied in some detail from different viewpoints that include: climate-vegetation relationships (Ern, 1972; Vogelmann, 1973; Lauer, 1978; Maderey *et al*., 1989; Holwerda *et al.*, 2010; Esperón-Rodríguez and Barradas, 2015), hydrological balance (Barradas, 1983; Gotsch *et al.*, 2014), chemical characteristics and effects of fog water deposition (Báez *et al*., 1998), and some meteorological (Fitzjarrald, 1986) and microphysical aspects (García-García and Montañez, 1991; García-García *et al*., 2002). For the Mexico Basin, Magaña *et al.* (2002) explored the general characteristics of fog formation and its consequences for the international airport operations. To the best of our knowledge, there are no other comprehensive fog studies, either on the national or regional scale, exception made of a climatology for Mexico developed by García-García and Zarraluqui (2008) based on observational records from climatological stations, which also includes a detailed fog occurrence study for the two regions mentioned above.

Mexico City – located in the Mexico Basin, at the southern end of the Central Plateau – concentrates the highest nation's population density, and the largest share of the gross domestic product. The Mexico Basin covers an area of about 30 km in radius roughly centered at downtown Mexico City (19°26′N, 99°08′W) and at an average altitude of 2,240 m above mean sea level (a.m.s.l.). The basin is mostly surrounded by mountains, including some of the highest peaks in the country, except o the northeast. This latter area is the location of Mexico City's International Airport – the major airport in the country – and was originally occupied by Lake Texcoco, the largest of a system of interconnected lakes in the basin that have been systematically drained over the last four hundred years (Jáuregui, 2000). Depending on the season, different synoptic and mesoscale features prevailing in the region – that are modified by the local orography and aided by the additional local source of low-level atmospheric humidity provided by the remnants of Lake Texcoco – produce various types of fog episodes throughout the year. These characteristics pose a challenge for the modeling and forecasting of fog. According to García-García and Zarraluqui (2008), fog events in the Mexico Basin are not very frequent, reaching average maximum values of up to 7 fog days per month, but have important economic impacts on the airport operation. Unfortunately, the available climatology for the Mexico Basin does not include a characterization by fog type, necessary to better simulate and predict its occurrence.

The present study has two main purposes. First, to develop a detailed climatology of fog occurrence for the Mexico Basin that considers the meteorological origin of the events. And second, using this fog characterization, to examine the ability of the Weather Research and Forecasting (WRF) model (Wang *et al*., 2016) to simulate the formation and development of fog events in the region. The paper has been organized as follows: the Data and Methods section presents a general description of Mexico´s geographic and atmospheric characteristics that determine the formation of fog in the Mexico Basin; followed by a depiction of the methodology used for the characterization of fog types, and of the WRF model configurations used. Next, the Results and Discussion section analyzes the WRF modeling performance and the physical mechanisms involved in the formation and development of the different fog types simulated. The final section covers the conclusions.

DATA AND METHODS

The Study Region

Mexico is located in the southern half of North America, and is surrounded to the east by the Gulf of México and to the west by the Pacific Ocean. Its territory is a long strip of land extending between 14°30'N and 32°50'N, and is crossed by large mountain ranges with extensive plateaus in between (Fig. 1). These geographical characteristics have a large influence on air temperature, precipitation distribution and general circulation patterns, which result in a great variety of climatic regimes. The most outstanding feature of Mexico's orography is its Central Plateau, with an average elevation over 1,500 m a.m.s.l. On the western edge of the Plateau, high terrain forms a wide and complex cordillera roughly oriented from north-northwest to south-southeast, called Sierra Madre Occidental; and on its Eastern edge, almost parallel to the Gulf of Mexico, lies the Sierra Madre Oriental. The southern edge of the Plateau is marked by a belt of volcanoes that extends from west to east between latitudes 19°N and 20°N, called Eje Volcánico Transversal, where there are many small lacustrine basins separated by volcanic ridges at an average elevation of about 2,200 m a.m.s.l. The Mexico Basin is located in this latter area, which is a tropical highland subject to both wind systems above and lower air currents on its flanks (Mosiño-Alemán and García, 1974). During the winter, weather phenomena over the Plateau are determined by midlatitude systems. Accordingly, the latitudinal position

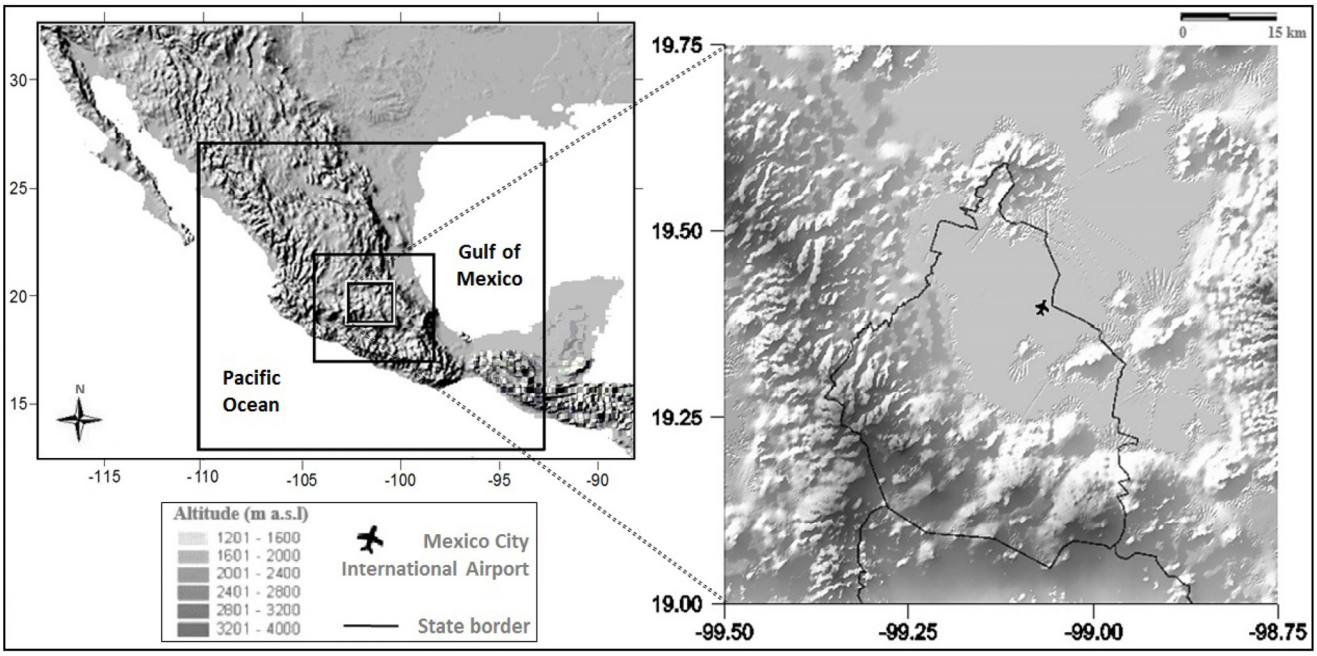

Fig. 1. Left: Relief map depicting the main orographic systems of Mexico and the three nested domains (27 km, 9 km and 3 km grid spacing) used for the numerical simulations. Right: Map of the Mexico Basin that coincides with the 3-km grid domain. See text for details.

of the large upper air currents is responsible for the duration and intensity of seasonal phenomena, like the rainy season and the degree of dryness of the cold season; whereas more transitory circulations have their seat in the lower levels of the atmosphere and, hence, are strongly influenced by orography. Thus, from the point of view of its rainfall regime – the rainy season occurs between May and October –, the climate of the Mexico Basin can be considered tropical and tempered by altitude (Jáuregui, 2000).

The synoptic and mesoscale systems which prevail in the Mexico Basin and influence the development of fog have been described in detail by García-García and Zarraluqui (2008), and are summarized in the following. In the summer, most of the Mexican territory gets under the influence of the trade winds along the south-western end of the semi-permanent Bermuda high-pressure system. These easterly winds gather humidity over the Gulf of Mexico and are orographically forced to ascend to higher altitudes, reaching the Central Plateau. On the western coast the circulation pattern is very much dependent on the dynamics of the intertropical convergence zone, since the development of a warm water pool over the northeast Pacific Ocean induces a region of deep convection and propitiates the formation of hurricanes that affect the Mexican coast and, in many occasions, reach the Central Plateau. On the other hand, in the winter the region lies in the Subtropical High and the synoptic situation is dominated by a deep trough in low latitudes that defines an elongated area of relatively low atmospheric pressure along its axis or trough line. This large-scale trough may include one or more closed circulations of low pressure, or cyclones, that produce northeasterly cold frontal systems which blow towards the shores of the Gulf of Mexico and towards the southern end of the Central Plateau. As mentioned before, in the Mexican Basin the rainy season occurs during summer and fall. Thus, it is not surprising that the least number of fog days in the year occurs in spring, with a minimum in March and April. The occurrence of fog increases towards the end of spring, coinciding with the beginning of the rainy and hurricane seasons in both coastal areas of the country (in May on the Pacific coast, and in June on the Atlantic-Caribbean coast). The available sources of humidity during summer (maximum incidence of hurricanes and peak of the rainy season) also coincide with a secondary maximum in the seasonal frequency of fog days in the Basin. Autumn marks the transition between the end of the hurricane season and the beginning of the season of cold frontal systems, thus producing a second minimum in fog occurrence. During winter, the frontal systems described above advect cold air towards the central Mexican Plateau, the flow being modified by the local orography, reaching the Mexico Basin and producing typical frontal fog episodes. Fog occurrences are more common in the northeastern zone of the Mexico Basin, where the international airport is located. In general, fogs form overnight when the mountain-valley circulation drains cool, humid air to the lower lands. As the day passes by, solar radiation warms up the lower atmospheric layers and the fog dissipates within a few hours after sunrise. It is also evident, however, that these relative fog-occurrence maxima are associated to local terrain features that modify and reinforce the synoptic and mesoscale circulation. For the airport area, the additional presence of small water bodies like the remnants of Lake Texcoco provides an additional local source of low-level atmospheric humidity.

It is clear that, depending on the prevailing circulation conditions, the fog episodes in the Mexico Basin can be of

various types. In the following section, a characterization by fog type is realized with the aim of determining which set of parameterizations is more suitable for their modeling in the region.

Fog Characterization

Given the synoptic and mesoscale characteristics discussed in the previous section, the classification of fog events in the Mexico Basin was accomplished by considering the typical atmospheric conditions observed in the three basic fog types. As mentioned before, a frontal fog is always associated with frontal zones and frontal passages, and can occur in a number of situations: when rain falling into cold stable air raises the dew point; when warm and cold air masses, each near saturation, are mixed by very light winds in the frontal zone; when relatively warm air is suddenly cooled over moist ground with the passage of a well-marked precipitation cold front; or when evaporation of frontal-passage rain water cools the surface and overlying air and adds sufficient moisture to form fog. Advection fog forms primarily through boundary layer dynamic and adiabatic processes, and is dominated by synoptic-scale processes that affect the lifetime of the event. Although radiative processes still play a role in its development and life cycle, they are not dominant so its formation can occur with light to moderate winds in the low levels. So, advection fogs are characterized by a temperature inversion near the surface, weak to moderate surface wind, surface wind shear and dry warm advection above the fog layer. Radiation fogs in the Mexico Basin form under the influence of the mountain-valley circulation and may be confused with an advection fog. In the latter, however, large-scale mass transport dominates the situation, whereas radiation fogs are favored in an environment with a large-scale low-level high pressure system, a temperature inversion in the fog layer, calm or light boundary-layer winds, high relative humidity near the surface, wet soil at the surface, and both wind shear and dry air above the fog layer.

The characterization of fog episodes according to their formation mechanisms was realized using ten years (2003–2012) of climatological data. These included aeronautical reports, meteorological bulletins, and atmospheric soundings. The methodology used is depicted in Fig. 2 and described in the following. First, each fog episode during the study period, regardless of its type, was identified using the Météorologique Aviation Régulière (METAR) reports issued for Mexico City's International Airport (available at http://vortex.plymouth.edu/myo/sfc/statlog-a.html). They consist of surface meteorological observations performed, recorded and transmitted at least once each hour in airports around the world (WMO, 2008), and include visual observations of fog occurrence within 15 km of the site. Second, the corresponding meteorological bulletins issued daily by the Mexican Weather Service (available at http://smn.cna.gob.mx/es/pronosticos/avisos) that contain the prevailing meteorological observations, synoptic charts and satellite images, were inspected to look for the presence of synoptic or mesoscale systems.

If the passage of a front in the Basin was reported – more commonly cold fronts during autumn and winter –, the episode was characterized as a frontal fog. Otherwise, the report of any other synoptic or mesoscale system advecting moisture from the oceans towards the Central Plateau at low atmospheric levels – typically those associated to African easterly waves and tropical cyclones near the coasts, and to systems embedded in those waves as clusters of convective clouds – or of a low-level anticyclone with clear skies were the first instance criteria used to classify the event as an advection or a radiation fog, respectively. Finally, radiosonde observations (available at http://weather.uwyo.edu/upperair/sounding.html) made twice a day at 00Z and 12Z at the National Observatory of Tacubaya – located approximately 12 km to the southwest of the airport – were analyzed to determine vertical profiles of temperature, mixing ratio and

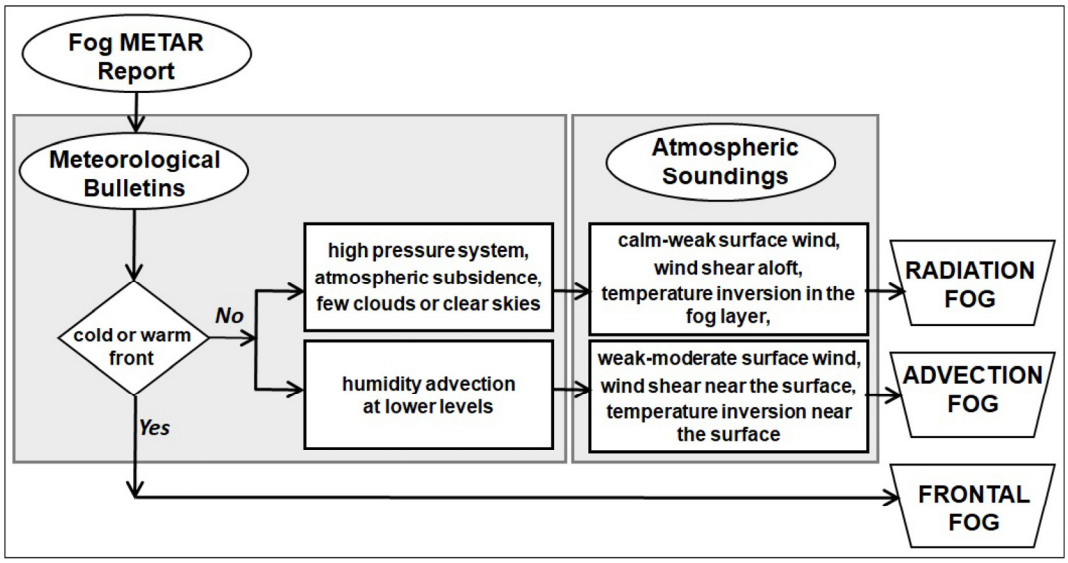

Fig. 2. Schematic diagram depicting the methodology for classifying events as advection, radiation or frontal fogs. See text for details.

wind, and to make a final decision on the type of fog present, i.e., either advection or radiation fog (see Fig. 2).

WRF Model

Modeling of fog episodes in the Mexico Basin was realized using the Weather Research and Forecasting (WRF) model version 3.1 – a widely used, next-generation mesoscale numerical weather prediction system designed for both atmospheric research and operational forecasting (Wang *et al*., 2016) – over a region covering central-southern Mexico, centered at Mexico City International Airport (19°26′N, 99°04′W), and integrated using three nested domains with 27 km, 9 km and 3 km grid spacing (see Fig. 1). Terrain and land cover data were obtained from the United States Geological Survey database (USGS, 2012). The vertical WRF model domain consisted of 42 layers, 23 of them assigned to the lowest 2,100 m from the ground. The National Centers for Environmental Prediction Global Forecast System data (GFS – NCEP, 2015), available with a 0.5° × 0.5° horizontal resolution, provided initial and boundary conditions. The model uses one-way nested boundary conditions in all three domains. The outer domain is updated every 6 hours with the GFS-NCEP forecast. Each simulation was of 30 hours, but only the last 18 hours were considered for analyses the first 12 hours left for the dynamical adjustment of the model (Wang *et al*., 2016).

To find out which model physical processes setups rendered the best results for each type of fog, several experiments were realized using different combinations of parameterizations. Nine representative cases – three for each fog type – were chosen to test each of the ten combinations presented in Table 1, so about 90 runs of the model were realized. The schemes tested were: for cloud microphysics, the Single-Moment 3-Class and 5-Class (WSM3 and WSM5 – Hong *et al*., 2004), the Eta-Ferrier (Rogers *et al*., 2001), the Kessler (1969), and the CAM 5.1 (Neale *et al*., 2012); for the planetary boundary layer (PBL), the Yonsei University (YSU – Hong *et al.*, 2006), the Mellor-Yamada-Janjić (Janjić, 1994), and the Quasi-Normal Scale Elimination (QNSE – Sukoriansky *et al*., 2005). Two surface schemes were used: a 5-layer thermal diffusion surface scheme (Dudhia, 1996), and the more complex Noah Land Surface Model (Chen and Dudhia, 2001) that consists of four soil layers and a vegetation layer on top. These two schemes are very similar and only vary in the degree of complexity (Ek *et al*. 2003). From these sensitivity tests, two different configuration combinations were chosen: one for radiation fog, and another for frontal and advection fog simulations. The cloud microphysics and planetary boundary layer (PBL) schemes used for frontal and advection fogs experiments were, respectively, the WSM3 and the YSU; whereas for radiation fog simulations, the CAM 5.1 cloud microphysics and the PBL QNSE schemes were chosen.

The WSM3 scheme considers three categories of hydrometeors: water vapor, water and ice cloud, and rain and snow (Hong *et al*., 2004). The cloud water-rain and the cloud ice-snow are assumed for temperatures above and below 0°C, respectively; and thus this scheme shows better results for fog simulations in the Mexico Basin, where minimum average temperatures in the coldest part of the year are greater than 1°C (Jáuregui, 2000). On the other hand, the CAM 5.1 scheme shows to be more appropriate for radiation fog simulation, the reason being that it allows for the tuning of threshold relative humidity for low and high clouds (78.75% and 80% were set over land without snow, respectively), and interpolated thresholds for the mid-level clouds. In this way, this parameterization produces condensation and evaporation for subgrid clouds with changing cloud fraction (Rasch and Kristjánsson, 1998; Park *et al.*, 2014), even if the subgrid is sub-saturated (Ma *et al*., 2014). As for the PBL schemes, the QNSE uses a theory of turbulence with stable and weakly unstable stratification that accommodates the stratification-induced disparity between the transport processes in the horizontal and vertical directions, and accounts for the combined effect of turbulence and waves. It predicts various important characteristics of stably stratified flows, such as the dependence of the vertical turbulent Prandtl number on Froude and Richardson numbers, anisotropization of the flow filed, and decay of vertical diffusivity under strong stratification (Sukoriansky, 2005). Finally, the Noah Land Surface Model was chosen for all numerical experiments because it better replicated land use conditions in the study area.

RESULTS AND DISCUSSION

Climatology

The average annual frequency of fog occurrence in the

Table 1. Parameterizations and schemes combinations tested for the numerical simulations using WRF.

Scheme Combination	Cloud Microphysics	Planetary Boundary Layer	Land Surface
1	Single-Moment 3-Class	Mellor–Yamada–Janjić	Noah Land Surface Model
2	Single-Moment 3-Class	Yonsei University Scheme	5-Layer Thermal Diffusion Scheme
3	Single-Moment 3-Class	Yonsei University Scheme	Noah Land Surface Model
4	Single-Moment 5-Class	Mellor–Yamada–Janjić	5-Layer Thermal Diffusion Scheme
5	Single-Moment 5-Class	Mellor–Yamada–Janjić	Noah Land Surface Model
6	Single-Moment 5-Class	Yonsei University Scheme	Noah Land Surface Model
7	CAM 5.1 Scheme	Quasi-Normal Scale Elimination	Noah Land Surface Model
8	Ferrier Scheme	Yonsei University Scheme	Noah Land Surface Model
9	Kessler Scheme	Mellor–Yamada–Janjić	5-Layer Thermal Diffusion Scheme
10	Kessler Scheme	Mellor–Yamada–Janjić	Noah Land Surface Model

Mexico Basin was found to be 23 episodes per year, with a high interannual variability (standard deviation ~60%). The total number of occurrences per month and fog type over the ten-year period is shown in Fig. 3. Almost 12% of all cases corresponded to radiation fogs distributed over the year and showing a maximum in November. Advection fogs accounted for about 44% of all cases, with a maximum in July and minima in February and March. The remaining 44% of the cases were classified as frontal fogs, most of them in the autumn and winter months, with notorious maxima in November and December, and almost none occurring the rest of the year.

These results are consistent with those of García-García and Zarraluqui (2008), who obtained similar annual and seasonal values calculated from standard climate records for the 30-year period from 1961 to 1990. According to these authors, the rainy season in Central Mexico begins in May and lasts through October. Consequently, the occurrence of advection fogs increases towards the end of spring – coinciding with the beginning of the rainy season – due to the presence of mesoscale systems over the region. Autumn marks the transition between the end of the hurricane season and the beginning of the middle latitudes systems (cold fronts) affecting Mexico. These advect cold air towards central Mexico producing typical cold-front post-frontal and frontal-passage fog events. Thus, it is not surprising for frontal fog episodes to be more frequent during the dry season, and that no frontal fog events were found associated to the passage of warm fronts.

Independently of their type, most fog events form in the early morning, i.e., between 04:00 and 10:00 LST (local standard time), most commonly at around 07:00 hours. During the dry season, many fog events occur after the passage of cold fronts that leave behind moister air and light winds. The frequency of fog duration by type is shown in Fig. 4. About 90% of the episodes last nearly three hours, thus dissipating before noon. Most radiation fogs (almost 90%) lasted two or less hours, as the lower atmospheric layers warm up after sunrise. On the other hand, both advection and frontal fog episodes tend to last longer, indicating the influence of the predominating mesoscale and synoptic systems. In particular, 25% of advection fog episodes last more than two hours; and 40% of frontal fogs persist even longer, with a few events lasting up to seven hours.

From the radiosonde data, the height of the inversion and the thickness of the fog layer were also estimated. Their typical values, broken down by fog type and season, are summarized in Table 2. The characteristics of the inversion layer during the rainy season are similar to those obtained by Montañez and García-García (1993) during some extreme pollution episodes in Mexico City. As for the fog thickness, although 500 m was the value most commonly observed, it should be noticed that it can reach up to 1,500 m, particularly during the rainy season.

WRF Fog Modeling

Once the two different model configuration combinations were chosen, all 230 cases identified during the study period were simulated: 26 radiation fogs using the CAM 5.1/QNSE combination; and 204 advection and frontal fogs with the WSM3/YSU combination. For the sake of brevity, only the results obtained for three simulations representative of radiation, advection and frontal fog types are summarized in Figs. 5, 6 and 7.

For the radiation fog event, METAR data reported fog starting at 05:51 LST. Fig. 5(a) shows that the surface (2 m above the ground) temperature is under-predicted at day time before 03:00 LST, and then gradually over-predicted. At the time of fog formation, such over-prediction reaches about 2.5°C in comparison to METAR observational data,

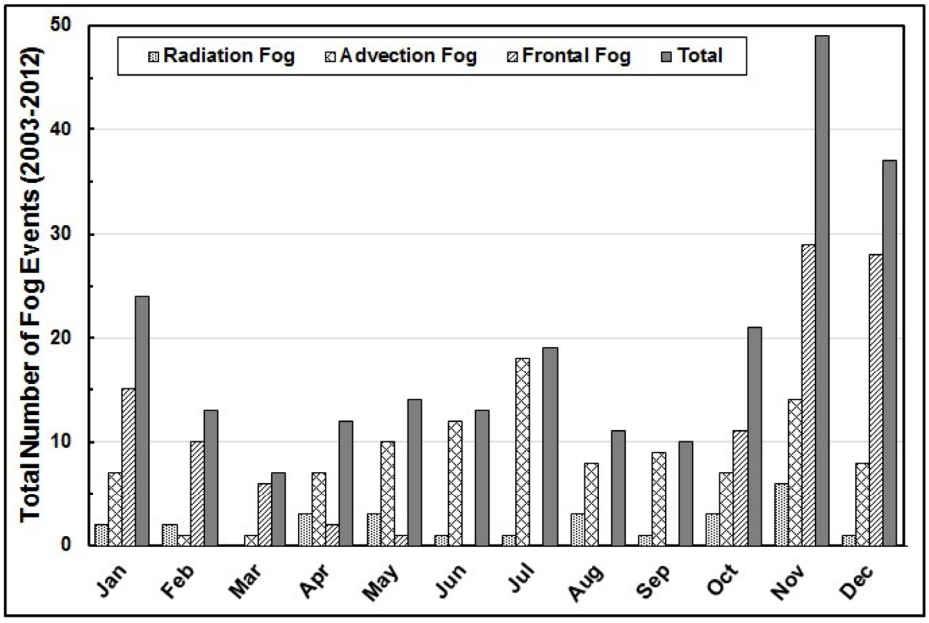

Fig. 3. Total number of fog events – broken down by month – in the Mexico Basin over the 2003–2012, ten-year period according to reports at Mexico City's International Airport METAR station.

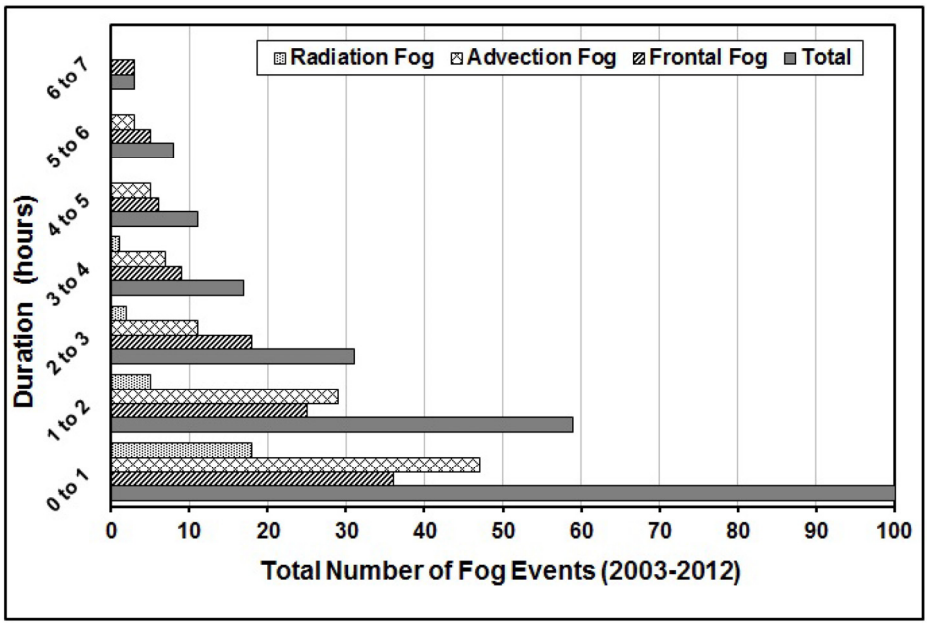

Fig. 4. Duration of fog episodes in the Mexico Basin over the 2003–2012, ten-year period, according to METAR reports at Mexico City International Airport.

Table 2. Characteristics of the inversion layer and fog thickness obtained with the radiosonde data.

Fog type	Season	Inversion layer (bottom) height (m)	Inversion layer temperature (°C)	Fog layer thickness (m)
Radiation	Rainy	0–900	1–5	10–1,000
	Dry	0–500	1–4	20–600
Advection	Rainy	15–400	2–6	10–1,500
	Dry	50–600	1–8	15–1,000
Frontal	Dry	0–500	1–8	10–1,500

whereas saturation seems to begin at around 80% relative humidity. The simulated fog thickness was around 250 m, as defined by the 0.10 g m^{-3} contour in Fig. 6(a), and cloud water spatial distributions at the 2-m level above the ground (Fig. 7(a)) coincide with the METAR fog reports. It is remarkable that both the formation and dissipation times were generally quite well simulated, and that the cloud liquid water content values obtained were of the same order of magnitude as observations reported by several authors (Jiusto, 1981).

The advection and frontal fogs cases – using a different WRF configuration – also showed very good results. The overestimation of surface temperature at the time of fog formation was slightly smaller than in the radiation fog case (about 2°C), and saturation also begins at around 80% relative humidity (Figs. 5(b) and 5(c)). The simulated fog thicknesses were, as it should be expected, larger: about 600 m and 1,500 m for the advection and frontal fogs, respectively (Figs. 6(b) and 6(c)). It is interesting to note that in all three simulations fog formation starts aloft (at a height of about 250 m for radiation and advection fogs, and about 800 m for frontal fog), then spreading up and downward to reach the ground after 30 to 60 minutes. Pagowski *et al*. (2004) found a similar behavior while simulating a dense advection fog occurrence in Canada, whereas Zhou and Ferrier (2008) indicated that this is due to the existence of certain turbulence near the ground. As in the radiation fog case, the results for the spatial distribution, and formation and dissipation times were also quite well reproduced (Figs. 7(b) and 7(c)).

CONCLUSIONS

A climatology by fog type for the Mexico Basin has been developed. The results indicate a high variability in the frequency of occurrence both by type and season, the latter well correlated with the dominant mesoscale and synoptic features. The WRF model with different physical processes parametrizations was used to investigate its skill to reproduce the formation of fog in the Mexico City International Airport area. It was found that the WSM3/YSU combination reproduced advection and frontal fog events quite well, whereas the CAM 5.1/QNSE combination worked better for radiation fog episodes. In all simulated cases, and in particular for advection and frontal fog events, the formation and dissipation times, thicknesses and spatial distributions were consistent with the observations. Best results were obtained when cloud microphysical parameterizations included both warm and cold rain processes. Particularly, the WSM3 parameterization (without supercooled water)

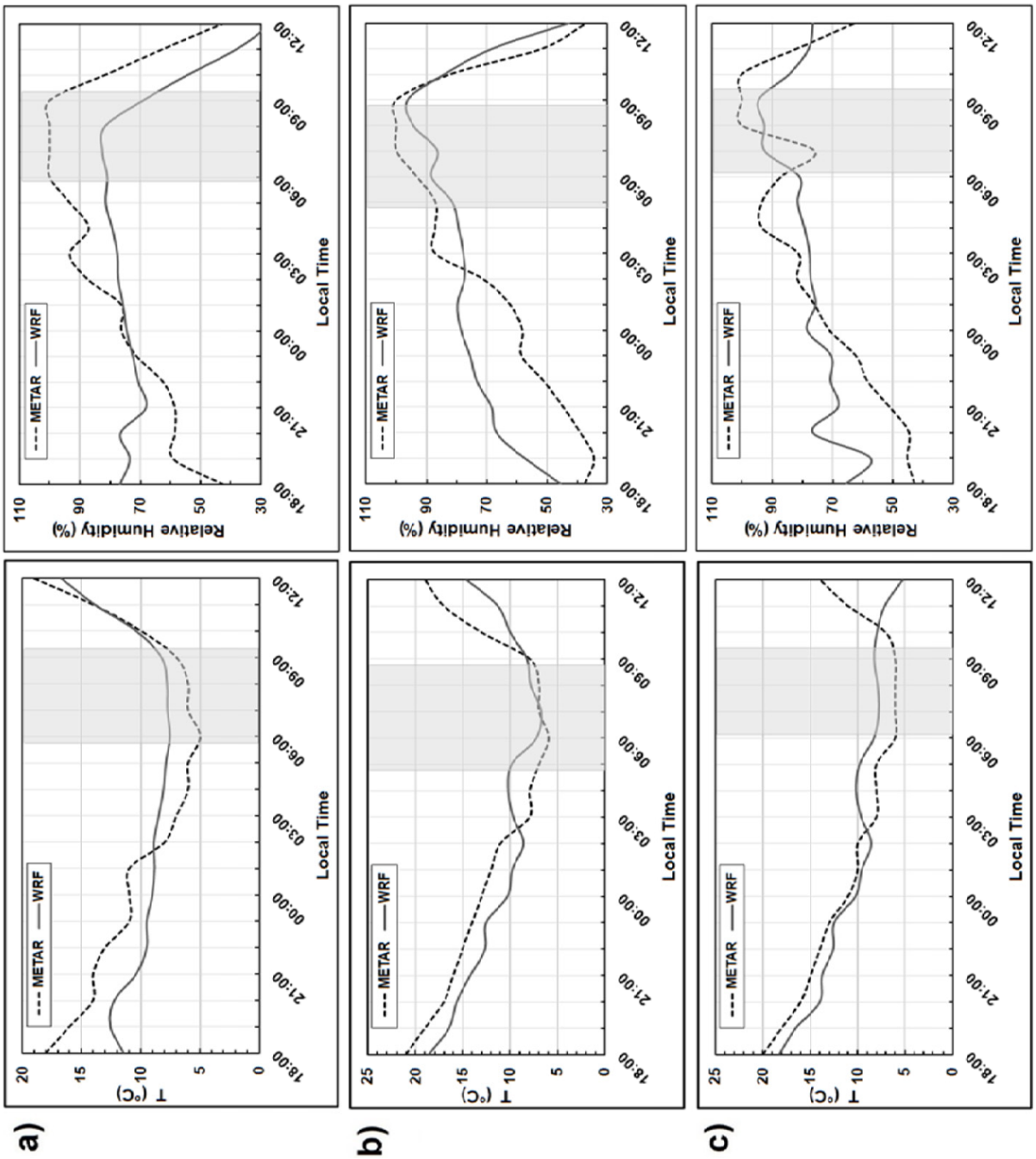

Fig. 5. Observed and simulated temperature (left panels) and relative humidity (right panels) at 2 m above the ground for three fog events. (a) Radiation fog on 26 November 2008, METAR formation - dissipation times: 05:51 LST–09:20 LST; (b) advection fog on 9 November 2012, METAR formation - dissipation times: 04:52 LST–08:51 LST; and (c) frontal fog on 2 January 2004, METAR formation - dissipation times: 06:10 LST–09:20 LST. The shaded area represents the fog period.

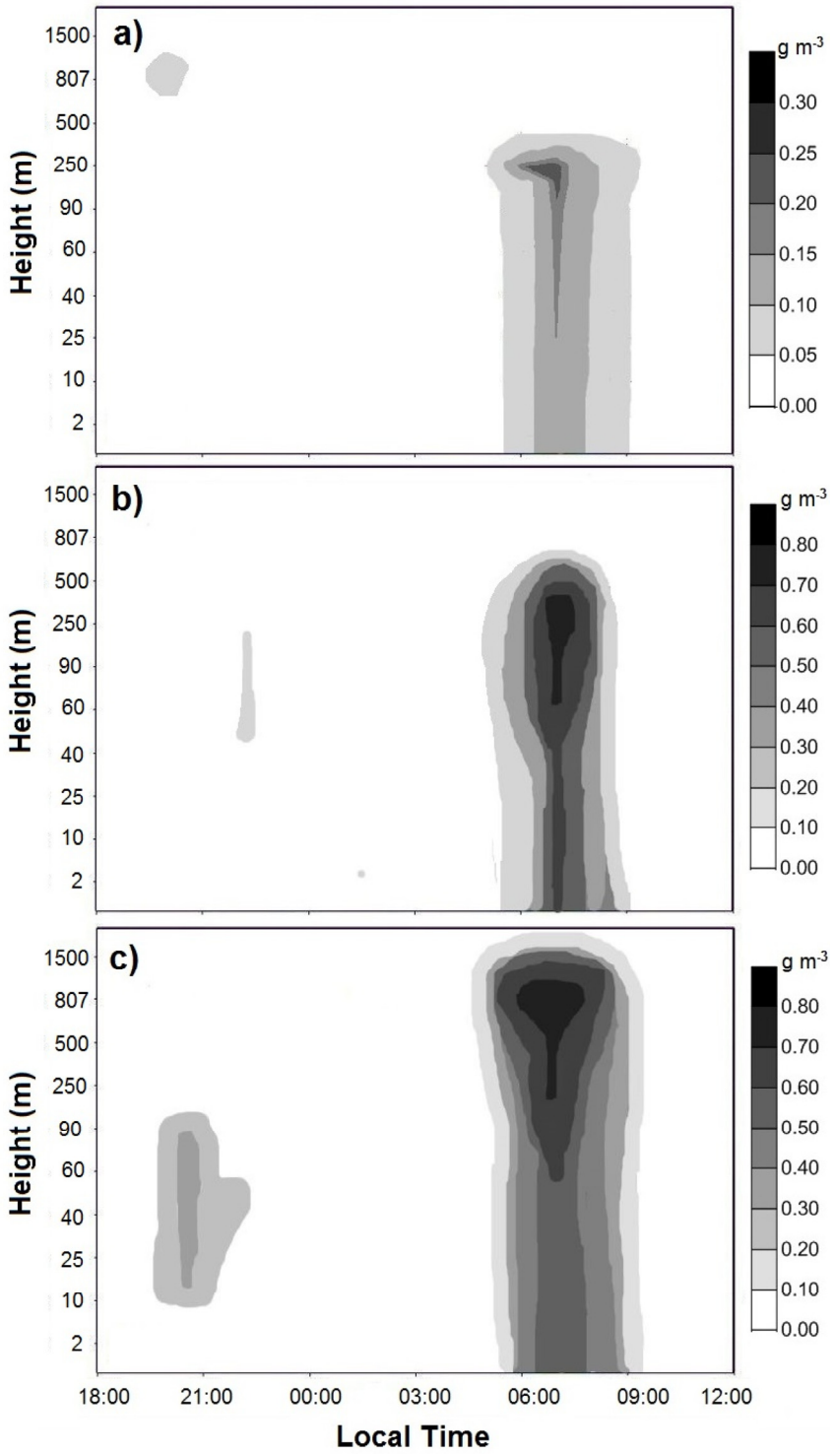

Fig. 6. Time evolution of vertical profiles of cloud liquid water content (in g m^{-3}), modeled at the Mexico City International Airport location, for the three fog events shown in Fig. 5. (a) Radiation fog; (b) advection fog; and (c) frontal fog. Notice the change in scale for cloud liquid water content between the radiation and the advection and frontal fog episodes.

inhibits ice processes, thus preventing frost formation and moisture deposition over the surface. In summary, the present study shows that the WRF model has the ability to simulate fog events in the Mexico Basin, provided that the appropriate physical processes configuration is used. Further research is needed to assess an operational fog forecast system for the region using the configurations proposed here. Given that none of the three different fog types found in the region is dominant, an ensemble forecasting system – as proposed by Zhou and Du (2010) – seems to be more suitable for this purpose. Such investigation is currently under way.

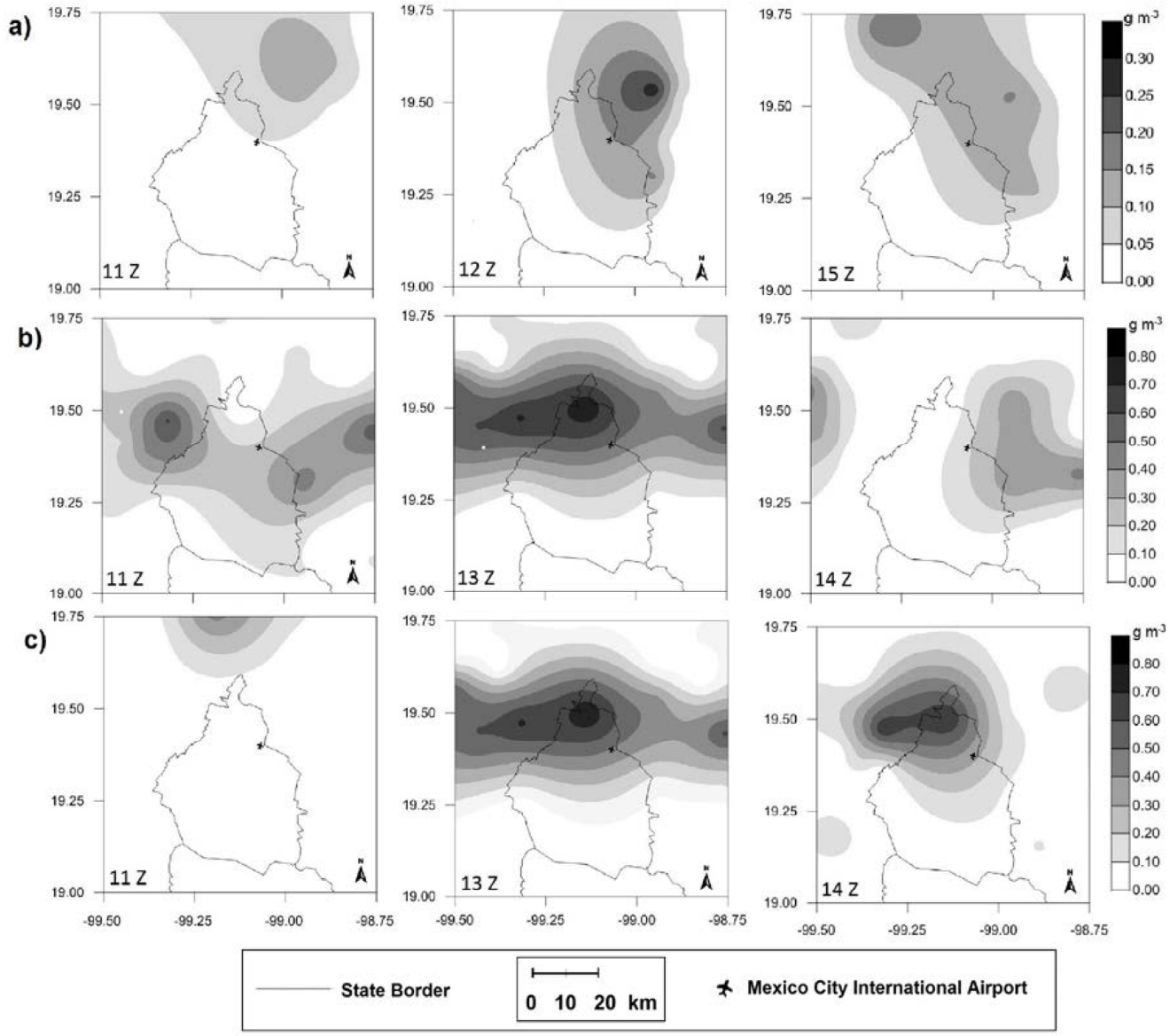

Fig. 7. Time series of spatial distribution (cloud liquid water content, in g m^{-3}, at 2 m above the ground) simulated for the three fog events shown in Fig. 5. (a) Radiation fog; (b) advection fog; and (c) frontal fog. Times shown on each panel correspond approximately, from left to right, to the formation, mature and dissipation stages. Notice the change in scale for cloud liquid water content between the radiation and the advection and frontal fog episodes.

ACKNOWLEDGMENTS

The authors wish to thank Mr. Víctor Zarraluqui for his help in the drawing of several of the figures. One of the authors (PGV) is indebted to Consejo Nacional de Ciencia y Tecnología (CONACyT) of Mexico for a graduate scholarship.

REFERENCES

AMS (2017). Fog. American Meteorological Society Glossary of Meteorology, http://glossary.ametsoc.org/wiki/Fog.

Báez, A.P., Padilla, H.G. and García-García F. (1998). Fog water chemistry at high altitudes in Mexico. Proc. First Int. Conf. Fog and Fog Collection, Schemenauer, R.S. and Bridgman, H. (Eds.), Vancouver, Canada, 1998, International Development Research Center, Ottawa, pp. 77–80.

Barradas, V.L. (1983). Capacidad de captación de agua a partir de la niebla en Pinus montezumae Lambert, de la región de las grandes montañas del estado de Veracruz. *Biótica* 8: 427–431.

Bergot, T. and Guédalia, D. (1994). Numerical forecasting of radiation fog. Part I: Numerical model and sensitivity tests. *Mon. Weather Rev.* 122: 1218–1230.

Bott, A. and Trautmann, T. (2002). PAFOG – A new efficient forecast model of radiation fog and low-level stratiform clouds. *Atmos. Res*. 64: 191–203.

Byers, H.R. (1959). *General meteorology*. McGraw-Hill,

New York.

Chen, F. and Dudhia, J. (2001). Coupling an advanced land surface-hydrology model with the Penn State-NCAR MM5 Modeling System. Part I: Model implementation and sensitivity. *Mon. Weather Rev.* 129: 569–585.

Choularton, T.W., Fullarton, G., Latham, J., Mill, C.S., Smith, M.H. and Stromberg, I.M. (1981). A field study of radiation fog in Meppen, West Germany. *Q. J. R. Meteorolog. Soc.* 107: 381–394.

Croft, P.J., Pfost, R.L., Medilin, J.M. and Johnson, G.A. (1997). Fog forecasting for the southern region: A conceptual model approach. *Weather Forecasting* 12: 545–556.

Dudhia, J. (1996). A multi-layer soil temperature model for MM5. Prepr. Sixth PSU/NCAR Mesoscale Model Users' Workshop, Boulder, Colorado, 1996, Mesoscale and Microscale Meteorology Division, National Center for Atmospheric Research, pp. 49–50.

Ek, M.B., Mitchell, K.E., Lin, Y., Rogers, E., Grunmann, P., Koren, V., Gayno, G. and Tarpley, J.D. (2003). Implementation of Noah land surface model advances in the National Centers for Environmental Prediction operational mesoscale Eta model. *J. Geophys. Res*. 108: 8851–8867.

Ern, H. (1972). Estudio de la vegetación en la parte oriental de México central. *Comunicaciones, Proyecto Puebla-Tlaxcala* 6: 1–6.

Esperón-Rodríguez, M. and Barradas, V.L. (2015). Ecophysiological vulnerability to climate change: Water stress responses in four tree species from the central mountain region of Veracruz, Mexico. *Reg. Environ. Change* 15: 93–108.

Fitzjarrald, D.R. (1986). Slope winds in Veracruz. *J. Clim. Appl. Meteorol.* 25: 133–144.

García-García, F. and Montañez, R.A. (1991). Warm fog in eastern Mexico: A case study. *Atmosfera* 4: 53–64.

García-García, F., Virafuentes, U. and Montero-Martínez, G. (2002). Fine-scale measurements of fog-droplet concentrations: A preliminary assessment. *Atmos. Res*. 64: 179–189.

García-García, F. and Zarraluqui, V. (2008). A fog climatology for Mexico. *Erde* 139: 45–60.

Gotsch, S.G, Asbjornsen, H., Holwerda, F., Goldsmith, G.R., Weintraub, A.E. and Dawson T.E. (2014). Foggy days and dry nights determine crown-level water balance in a seasonal tropical montane cloud forest. *Plant Cell Environ*. 37: 261–272.

Gultepe, I. (2007). *Fog and boundary layer clouds: Fog visibility and forecasting*. Pageoph Topical Volumes, Birkhauser Verlag Basel.

Gultepe, I. (2012). Fog and dew observations and modeling: Introduction. *Pure Appl. Geophys*. 169: 765–766.

Gultepe, I., Tardif, Michaelides, S.C., Cermak, J., Bott, A., Bendix, J., Müller, M.D., Pagowski, M., Hansen, B., Ellrod, G., Jacobs, W., Toth, G. and Cober, S.G. (2007). Fog research: A review of past achievements and future perspectives. *Pure Appl. Geophys*. 164: 1121–1159.

Gultepe, I., Bendix, J., Klemm, O., Eugster, W. and Cermak, J. (2012). *Fog and dew observations and modeling*. Pageoph Topical Volumes, Birkhauser Verlag Basel.

Gultepe, I., Zhou, B., Milbrandt, J., Bott, A., Li, Y., Heymsfield, A.J., Ferrier, B., Ware, R., Pavolonis, M., Kuhn, T., Gurka, J., Liu, P. and Cermak. J. (2015). A review on ice fog measurements and modeling. *Atmos. Res*. 151: 2–19.

Holwerda, F., Bruijnzeel, L.A., Muñoz-Villers, L.E., Equihua, M. and Asbjornsen, H. (2010). Rainfall and cloud water interception in mature and secondary lower montane cloud forests of central Veracruz, Mexico. *J. Hydrol.* 384: 84–96.

Hong, S.Y., Dudhia, J. and Chen, S.H. (2004). A revised approach to ice microphysical processes for the bulk parameterization of clouds and precipitation. *Mon. Weather Rev.* 132: 103–120.

Hong, S.Y., Yign, N. and Dudhia, J. (2006). A new vertical diffusion package with an explicit treatment of entrainment processes. *Mon. Weather Rev.* 134: 2318–2341.

Janjić, Z.I. (1994). The step-mountain Eta Coordinate Model: Further developments of the convection, viscous sublayer, and turbulence closure schemes. *Mon. Weather Rev.* 122: 927–945.

Jáuregui, E. (2000). *El clima de la ciudad de México*. Plaza y Valdés, Mexico City.

Jiusto, J. (1981). Fog structure. In *Clouds: Their formation, optical properties, and effects*. Hobbs, P.V. and Deepak, A. (Eds.), Academic Press, New York, pp. 187–239.

Kessler, E. (1969). On the distribution and continuity of water substance in atmospheric circulations, In *Meteorological monographs*, American Meteorological Society, Boston, MA, pp. 1–84.

Lauer, W. (1978). Tipos ecológicos del clima en la vertiente oriental de la Meseta Mexicana. *Comunicaciones, Proyecto Puebla-Tlaxcala* 15: 235–244.

Lee, Y.H., Lee, J.S., Park, S.K., Chang, D.E. and Lee H.S. (2010). Temporal and spatial characteristics of fog occurrence over the Korean Peninsula. *J. Geophys. Res*. 115: D14117.

Ma, P.L., Rasch, P.J., Fast, J.D., Easter, R.C., Gustafson Jr., W.I., Xiaohong, L., Ghan, S.J. and Singh, B. (2014). Assessing the CAM5 physics suite in the WRF-Chem model: implementation, resolution sensitivity, and a first evaluation for a regional case study. *Geosci. Model Dev*. 7: 755–778.

Maderey, R.L.E., del Castillo, H. and Cruz, F.J. (1989). Distribución del rocío y de la niebla: Fuentes de humedad para la vegetación en la República Mexicana. *Ciencia* 40: 223–231.

Magaña, V., García-Reynoso, A., Caetano, E., Jazcilevich, A., García-García, F. and Ruiz-Suárez, L.G. (2002). *Estudio preliminar para determinar el efecto en la formación de niebla y en la calidad del aire debido a la creación de cuerpos de agua en la ubicación del nuevo aeropuerto internacional de la ciudad de México*. Technical Report, Centro de Ciencias de la Atmósfera, Universidad Nacional Autónoma de México, Mexico

City.
Montañez, R.A. and García-García, F. (1993). Some urban and meteorological effects on the production of cloud condensation nuclei in Mexico City. *Atmosfera* 6: 39–49.
Mosiño-Alemán, P.A. and García, E. (1974). *The climate of Mexico*. In *Climates of north america*, Bryson, R.A. and Hare, F.K. (Eds.), Elsevier Scientific Publishing Company, Amsterdam-Lodon-New York, pp. 345–404.
Müller, M.D., Schmutz, C. and Parlow, E. (2007). A one-dimensional ensemble forecast and assimilation system for fog prediction. *Pure Appl. Geophys*. 164: 1241–1264.
Nakanishi, M, and Niino, H. (2006). An improved Mellor–Yamada level-3 model: Its numerical stability and application to a regional prediction of advection fog. *Boundary Layer Meteorol.* 119: 397–407.
NCEP (2015). NCEP GFS 0.25 Degree Global Forecast Auxiliary Grids Historical Archive, Research Data Archive at the National Center for Atmospheric Research, Boulder, Colo., http://dx.doi.org/10.5065/D6W09402.
Neale, R and co-authors (2012). Description of the NCAR Community Atmosphere Model (CAM5.0), NCAR/TN-486+STR, National Center for Atmospheric Research, http://www.cesm.ucar.edu/models/cesm1.0/cam/docs/description/cam5_desc.pdf.
Pagowski, M., Gultepe, I. and King, P. (2004). Analysis and modeling of an extremely dense fog event in Southern Ontario. *J. Appl. Meteorol.* 43: 3–16.
Park, S., Bretherton, C.S. and Rasch, P.J. (2014). Integrating cloud processes in the Community Atmosphere Model, version 5. *J. Clim*. 27: 6821–6856.
Rasch, P.J. and Kristjánsson, J.E. (1998). A comparison of the CCM3 Model Climate using diagnosed and predicted condensate parameterizations. *J. Clim*. 11: 1587–1614.
Rogers, E., Black, T., Ferrier, B., Lin, Y., Parrish, D. and Diego, G. (2001). Changes to the NCEP MesoEta Analysis and Forecast System: Increase in resolution, new cloud microphysics, modified precipitation assimilation, modified 3DVAR Analysis. Environmental Modeling Center, National Weather Service, National Centers For Environmental Prediction. http://www.emc.ncep.noaa.gov/mmb/mmbpll/eta12tpb/.
Román-Cascón, C., Yagüe, C., Sastre, M., Maqueda, G., Salamanca, F. and Viana, S. (2012). Observations and WRF simulations of fog events at the Spanish Northern Plateau. *Adv. Sci. Res.* 8: 11–18.
Román-Cascón, C., Steeneveld, G.J., Yagüe, C., Sastre, M., Arrillaga, J.A. and Maqueda, G. (2016). Forecasting radiation fog at climatologically contrasting sites: Evaluation of statistical methods and WRF. *Q. J. R. Meteorolog. Soc.* 142: 1048–1063.
Shimadera, H., Kondo, A., Shrestha, K.L., Kaga, A. and Inoue, Y. (2011). Annual sulfur deposition through fog, wet and dry deposition in the Kinki Region of Japan. *Atmos. Environ*. 45: 6299–6308.
Steppeler, J., Doms, G., Schättler, U., Bitzer, H.W., Damrath, A.G. and Gregoric, G. (2003). Meso-gamma scale forecasts using the nonhydrostatic model LM. *Meteorol. Atmos. Phys*. 82: 75–96.
Sukoriansky, S., Galperin, B. and Perov, V. (2005). Application of a new spectral theory of stably stratified turbulence to the atmospheric boundary layer over sea ice. *Boundary Layer Meteorol.* 117: 231–257.
USGS (2012). Central American Land Cover Data, The USGS Land Cover Institute, http://landcover.usgs.gov/landcoverdata.php#ca
Van der Velde, I.R., Steeneveld, G.J., Wichers Schreur, B.G.J. and Holtslag, A.A.M. (2010). Modeling and forecasting the onset and duration of severe radiation fog under frost conditions. *Mon. Weather Rev.* 138: 4237–4253.
Vogelmann, H.W. (1973). Fog precipitation in the cloud forests of eastern Mexico. *BioScience* 23: 96–100.
Wang, W., Bruyère, C., Duda, M., Dudhia, J., Gill, D., Kavulich, M., Keene, K., Lin, H.C., Michalakes, J., Rizvi, S., Zhang, X., Berner J. and Fossell, K. (2016). *ARW version 3 modeling system user's guide*, Mesoscale & Microscale Meteorology Division, National Center for Atmospheric Research, http://www2.mmm.ucar.edu/wrf/users/docs/user_guide_V3/ARWUsersGuideV3.pdf.
Willett, H.C. (1928). Fog and haze, their causes, distribution, and forecasting. *Mon. Weather Rev.* 56: 435–468.
WMO (1992). *International meteorological vocabulary*, WMO-No.182, second edition, Secretariat of the World Meteorological Organization, Geneva.
WMO (2008). *Aerodrome reports and forecasts: A users' handbook to the codes*, WMO No.782, Secretariat of the World Meteorological Organization, Geneva.
Zhou, B. and Ferrier, B.S. (2008). Asymptotic analysis of equilibrium in radiation fog. *J. Appl. Meteorol. Climatol.* 47: 1704–1722.
Zhou, B. and Du, J. (2010). Fog prediction from a multimodel Mesoscale Ensemble Prediction System. *Weather Forecasting* 25: 303–322.
Zhou, B., Du, J., Gultepe, I. and Dimego, G. (2012). Forecast of low visibility and fog from NCEP: Current status and efforts. *Pure Appl. Geophys*. 169: 895–909.

Received for review, December 12, 2016
Revised, July 13, 2017
Accepted, July 14, 2017